

Article

Plasmodium falciparum Nicotinamidase as A Novel Antimalarial Target

Dickson Donu¹, Chiranjeev Sharma¹  and Yana Cen^{1,2,*}¹ Department of Medicinal Chemistry, Virginia Commonwealth University, Richmond, VA 23219, USA² Institute for Structural Biology, Drug Discovery and Development, Virginia Commonwealth University, Richmond, VA 23219, USA

* Correspondence: ceny2@vcu.edu; Tel.: +1-804-828-7405

Abstract: Inhibition of *Plasmodium falciparum* nicotinamidase could represent a potential antimalarial since parasites require nicotinic acid to successfully recycle nicotinamide to NAD⁺, and importantly, humans lack this biosynthetic enzyme. Recently, mechanism-based inhibitors of nicotinamidase have been discovered. The most potent compound inhibits both recombinant *P. falciparum* nicotinamidase and parasites replication in infected human red blood cells (RBCs). These studies provide evidence for the importance of nicotinamide salvage through nicotinamidase as a central master player of NAD⁺ homeostasis in *P. falciparum*.

Keywords: *P. falciparum*; nicotinamidase; antimalarial; NAD⁺ homeostasis

**Citation:** Donu, D.; Sharma, C.;Cen, Y. *Plasmodium falciparum*

Nicotinamidase as A Novel

Antimalarial Target. *Biomolecules*2022, 12, 1109. [https://doi.org/](https://doi.org/10.3390/biom12081109)

10.3390/biom12081109

Academic Editors: Giovanni

N. Roviello and Caterina

Vicidomini

Received: 4 July 2022

Accepted: 11 August 2022

Published: 12 August 2022

Publisher's Note: MDPI stays neutral with regard to jurisdictional claims in published maps and institutional affiliations.



Copyright: © 2022 by the authors. Licensee MDPI, Basel, Switzerland. This article is an open access article distributed under the terms and conditions of the Creative Commons Attribution (CC BY) license (<https://creativecommons.org/licenses/by/4.0/>).

1. Introduction

Nicotinamidases are metabolic enzymes that catalyze the hydrolysis of nicotinamide (NAM) to nicotinic acid (NA) [1,2]. NAM is the reactive moiety within the dinucleotides NAD(H) and NADP(H). The conversion of free NAM to NA catalyzed by nicotinamidase enables cells to recycle this moiety, leading to the re-conjugation of pyridine-3-carboxylate and ribose-5-phosphate to form nicotinic acid mononucleotide (NaMN), and eventual reformation of NAD⁺ (Figure 1). Nicotinamidases are widely distributed in biology, and are found ubiquitously in archaea, mycobacteria, eubacteria, and in unicellular and multicellular eukaryotes, but not in mammals [1,3–10]. The fact that nicotinamidases are not found in human cells, but appear in numerous pathogens that infect humans, suggests that nicotinamidases could be the targets of novel antimicrobials.

To better understand the feasibility of targeting nicotinamidase as an antimicrobial strategy in general, and how it might be of particular effect in treating *P. falciparum* infection, it is instructive to consider the general organization of a complete NAD⁺ metabolism in microbes (Figure 1) and how it contrasts with humans (Figure 2). The typical pathways that converge to NAD⁺ are divided into several components. These are widely designated de novo and salvage pathways [3,4,7,11]. All known de novo pathways require the formation of quinolinate (Figures 1 and 2). Quinolinate is the precursor of the biosynthetic intermediate NaMN which implies that NA is not formed as a free compound in the de novo pathway. NaMN is then adenylated to nicotinic acid adenine dinucleotide (NaAD) and further acted upon by ATP-dependent NAD⁺ synthetase to form NAD⁺. Both microbes and humans have this pathway. Because of the overlapping of these pathways, the identification of highly selective inhibitors that do not affect human enzymes has been a major concern, even though enzymes such as nicotinate mononucleotide adenyltransferase [12,13] and NAD⁺ synthetase [14,15] have been identified as potential targets for antimicrobials.

Salvage pathways are known to reconstitute NAD⁺ from metabolites that already incorporate a finished NAM or NA ring within the compound. Within most organisms, the NAM and NA pathways are overlapping, with the enzyme nicotinamidase required to convert NAM to NA (Figure 1A) [3,7]. A nicotinic acid phosphoribosyltransferase

(NAPRTase) is responsible for resynthesis of NaMN, with the remaining steps common to the *de novo* pathway. The corresponding strategy of human metabolism is different. NAM is directly recycled by nicotinamide phosphoribosyltransferase (NAMPT) that couples it to 5-phospho-ribose-1-pyrophosphate (PRPP) to form nicotinamide mononucleotide (NMN, Figure 1B) [11,16], a mechanism first recognized by Detrich et al. in 1966 [17]. NA is recycled to form NaMN, in what is known as the Preiss–Handler pathway, [18] reaching a common intermediate of the *de novo* pathway [8,19]. Importantly, human NAD⁺ metabolism is not known to create NA as a free species. It is thought that NA originates mostly from dietary sources and is not synthesized in cells [8,19]. Because NAM is formed readily from rapid NAD⁺ turnover in mammalian cells, the most prevalent precursor to make NAD⁺ in the body is NAM. Importantly, the only salvage enzyme that is unique to pathogens is nicotinamidase, suggesting that if microbes are heavily reliant on this enzyme for NAD⁺ biosynthesis, it could be an effective antimicrobial target.

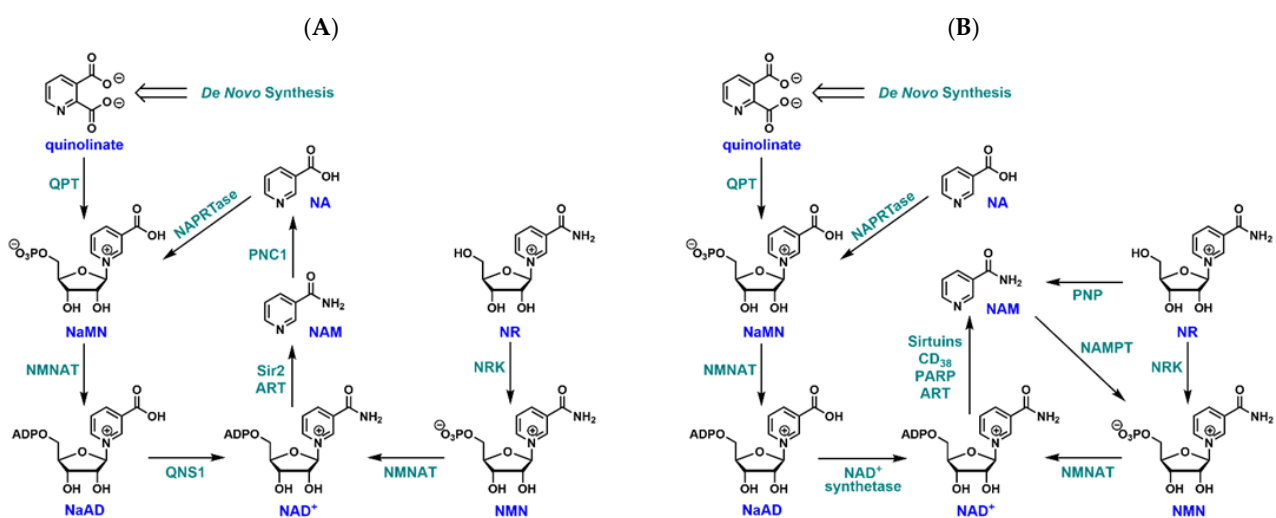


Figure 1. Comparison of NAD⁺ biosynthetic pathways. (A) NAD⁺ metabolism in most bacteria, yeast and multicellular eukaryotes. NA: nicotinic acid; NAM: nicotinamide; NR: nicotinamide riboside; NMN: nicotinamide mononucleotide; NaMN: nicotinic acid mononucleotide; NaAD: nicotinic acid adenine dinucleotide; QPT: quinolinate phosphoribosyltransferase; PNC1: nicotinamidase; QNS1: glutamine-dependent NAD⁺ synthetase; NRK: nicotinamide riboside kinase; ART: ADP-ribose transferase; NMNAT: nicotinamide mononucleotide adenyltransferase. (B) NAD⁺ biosynthetic pathways in mammals. There is a lack of nicotinamidase, no direct path for converting nicotinamide to nicotinic acid. NAMPT: nicotinamide phosphoribosyltransferase; PNP: purine nucleoside phosphorylase; PARP: poly(ADP-ribose) polymerase.

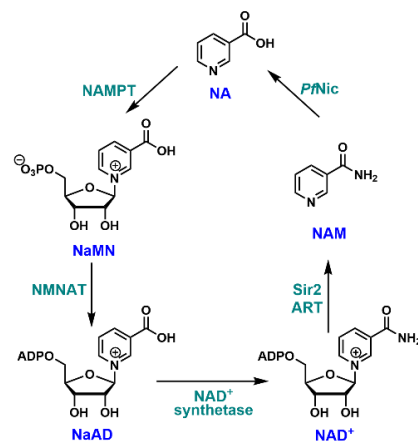


Figure 2. NAD⁺ biosynthetic pathways in *P. falciparum* as identified by activity, transcriptome, and genome studies on the organism.

The protozoan parasite *Plasmodium falciparum* causes the most severe form of human malaria and utilizes antigenic variation to avoid antibody recognition, resulting in greatly extended periods of infection [20–22]. Drug resistance is widespread [23–25], and novel agents against new targets are needed to support combination-therapy approaches promoted by the World Health Organization (WHO) [26,27]. The pathways of NAD⁺ metabolism in *P. falciparum* have not been extensively characterized, but genome and transcriptome analyses indicate that the NAD⁺ metabolism of this microbe is restricted to NA and NAM salvage pathways (Figure 2) [28–30]. Because *P. falciparum* has nicotinamidase and nicotinate phosphoribosyltransferase (NPT), it has been suggested that it can utilize either NA or NAM as the NAD⁺ source [30]. However, given that human cells do not directly make free NA and that NAM is abundant in mammalian tissues and in cells [31,32], *P. falciparum* has been implied to be highly dependent upon nicotinamidase activity for NAD⁺ synthesis. Consistent with this notion, *P. falciparum* infected erythrocytes express high levels of nicotinamidase, and have NAD⁺ contents 10 times higher than uninfected cells [33]. In support of the hypothesis that nicotinamidase activity is required for the bulk of NAD⁺ synthesis in *P. falciparum*, we present the novel result that NAM is the preferred source of *P. falciparum* NAD⁺ biosynthesis, even in the presence of NA. The inhibition of *P. falciparum* nicotinamidase (*PfNic*) has a significant adverse effect on NAD⁺ levels and parasite growth in cultures. Overall, our study suggests that *PfNic* serves as a viable antimalarial drug target.

2. Materials and Methods

2.1. Reagents and Instruments

All reagents were purchased from Sigma-Aldrich (St. Louis, MO, USA) or Fisher Scientific (Pittsburgh, PA, USA) and were of the highest purity commercially available. HPLC was performed on a Dionex Ultimate 3000 HPLC system equipped with a diode array detector using Macherey-Nagel C18 reverse-phase column. Radiolabeled samples were counted in a Beckman LS6500 scintillation counter. NMR spectra were acquired on a Bruker AVANCE III 500 MHz high-field NMR spectrometer, and the data were processed using Topspin software (https://www.bruker.com/en/products-and-solutions/mr/nmr-software/topspin.html?gclid=EAJalQobChMli-T93OvA-QIVzmSLCh2ScAJOEAAAYASAAEgLEgvD_BwE, accessed on 2 July 2022). Mass spectra were obtained with a Bruker Autoflex II MALDI-TOF mass spectrometer operated in positive ion reflectron mode. HRMS spectra were acquired with either a Waters Micromass Q-tof Ultima or a Thermo Scientific Q-Exactive hybrid Quadrupole Orbitrap.

2.2. Cloning and Expression of *PfNic* and Synthesis of Inhibitor

P. falciparum nicotinamidase was cloned, expressed, and purified as described previously [34]. 5-Me-nicotinaldehyde was synthesized according to previously published methods [34].

2.3. Parasite Culture

The chloroquine-sensitive *P. falciparum* strain 3D7 was cultivated at 5% hematocrit in RPMI 1640 medium, 0.5% Albumax II (Invitrogen, Waltham, MA, USA), 0.25% sodium bicarbonate, and 0.1 mg/mL gentamicin. Parasites were incubated at 37 °C in an atmosphere of 5% oxygen, 5% carbon dioxide and 90% nitrogen. Parasite cultures were synchronized using percoll/sorbitol gradient centrifugation as described previously [35]. Briefly, 3 mL of 40% percoll/6% sorbitol/RPMI 1640 medium was layered over 3 mL of 70% percoll/6% sorbitol/RPMI 1640 medium in a 15 mL centrifuge tube. Infected RBCs at 50% hematocrit were layered on top of the gradient. The gradient was then centrifuged at 12,000 × *g* for 20 min at room temperature. Highly synchronized parasites were recovered from the 40%/70% interface, washed twice with complete culture media. Microscopic evaluation of the recovered cells verify that they were >95% infected mature-stage parasites (trophozoites and schizonts). These cells were reconstituted with fresh RBCs and media.

Following erythrocyte invasion, the synchronized culture was used for drug or precursor treatment [36].

2.4. Inhibitor or NAD⁺ Precursor Treatment and NAD⁺ Measurements

Synchronized parasite cultures were treated with either inhibitor or NAD⁺ precursor at indicated concentrations. Media were changed every 12 h along with the chemicals. After a total of 48 h incubation, parasites were harvested using percoll/sorbitol gradient described above and washed twice with complete culture media. The pellets were then washed with 1 mL of PBS and were resuspended in 1 mL of PBS for cell counting using hemocytometer. After counting, the cells were centrifuged at 4000 rpm for 3 min at room temperature. To the pellets were added standard ¹⁸O-NAD⁺ (typically 1 nmol) and 70 µL of ice cold 7% perchloric acid [31,37–39]. The samples were vortexed for 30 s and sonicated on ice for 5 min. The vortex-sonication cycle was repeated three times. The samples were centrifuged at 14,500 rpm for 3 min at room temperature. The supernatant was taken out and neutralized to pH 7 with 3 M NaOH and 1 M phosphate buffer pH 9. The neutralized samples were centrifuged again at 14,500 rpm for 3 min. Clear supernatants were injected into HPLC to separate NAD⁺ from other cellular components. NAD⁺ peaks were collected according to the retention time of the authentic standard. Collections were lyophilized to dryness and subjected to MALDI-TOF analysis. Ratios of intensities for *m/z* = 664, 665, and 666 peaks, corresponding to unlabeled-, ¹⁵N-, and ¹⁸O-NAD⁺ isotopomers, were used to calculate NAD⁺ concentration in the sample. Corrections were applied for isotopic abundance.

2.5. Inhibition Study in Parasite Lysates

Synchronized parasites were incubated for 36 h under standard conditions (media were changed at the 24 h time point). Then they were treated with either vehicle (DMSO) or 50 µM 5-Me-nicotinaldehyde for 12 h. After a total of 48 h incubation (36 h drug free and 12 h drug-administrated), parasites were harvested using percoll/sorbitol gradient and washed twice with complete media. The pellets were then washed with 1 mL of PBS and were resuspended in 1 mL of PBS for cell counting using hemocytometer. After counting, the cells were centrifuged at 4000 rpm for 3 min at room temperature. To the pellets were added 60 µL of lysis buffer (50 mM Tris-HCl, pH 7.5, 5 mM EDTA and 1% Triton X-100), the pellets were gently suspended in the buffer. The samples were centrifuged at 4000 rpm for 3 min at room temperature. The supernatants were taken out and treated with 260,000 cpm of carbonyl ¹⁴C-nicotinamide for 30 min at 37 °C. Nicotinamide and nicotinic acid were separated and collected by HPLC, and radioactivity was determined by scintillation counting.

2.6. Luciferase Assay

The NF54-*luc* strain (a chloroquine sensitive line) expresses the *Renilla* luciferase gene under the control of the constitutively active *hrp3* promoter [40]. It was a generous gift from Dr. Kirk Deitsch (Weill Cornell Medical College). For viability assays, parasites were plated at 1–10% parasitemia in 96-well plates in standard media in the presence of the indicated concentrations of inhibitor. The total volume of culture was 200 µL and DMSO did not exceed 1% of the total culture volume. Media plus compounds were replenished every 12 h. After 48 h incubation, media were withdrawn, and RBCs were lysed with 100 µL of Bright-Glo Lysis Buffer (Promega, Madison, WI, USA). Lysates were then transferred to 96-well luminometer plates. To the lysates were added 100 µL of Bright-Glo *Renilla* Luciferase Reagent (Promega, Madison, WI, USA). Luminescence was measured immediately in a plate luminometer (Molecular Devices, San Jose, CA, USA). Each individual data point is represented in triplicate allowing determination of standard deviations. A broad range of compound concentrations are used to allow the determination of IC₅₀ value.

2.7. Preparation of Giemsa Stained Smears

Ready-to-use Giemsa stain solution (Sigma-Aldrich, St. Louis, MO, USA) was diluted 1:20 in phosphate buffer (pH~7). The blood smear was air-dried and fixed in methanol for 30 s. The slide was then placed in a staining jar containing the freshly made Giemsa working solution. The slide was stained for 15 min before it was rinsed in deionized water. The slide was then air-dried and observed with immersion oil.

3. Results

3.1. Essential Catalytic Residues Are Conserved in *P. falciparum* Nicotinamidase (PfNic)

Nicotinamidase has been found in numerous organisms. With the advent of genome sequencing, it is now possible to compare phylogenetic similarities of nicotinamidases derived from very different organisms (Figure 3). Common features of the nicotinamidases include a catalytic triad composed of a universally conserved Asp, found near the N-terminus of most nicotinamidases, a catalytic Cys, and a universally conserved Lys residue [34,41–45]. In addition, a feature of these active sites is a cis-peptide that creates the oxyanion hole that stabilizes tetrahedral intermediates generated during catalysis. Furthermore, a conserved metal ion binding site is found on all known nicotinamidases. Highly conserved His residues compose part of the binding site on all known nicotinamidase structures. For *S. cerevisiae* [44], *S. pneumoniae* [41], and *A. baumannii* [42], the metal bound is a transition metal ion, most likely Zn^{2+} . This ion has been proposed to be a Mn^{2+} or Mn^{2+}/Fe^{2+} for the *M. tuberculosis* nicotinamidase [43,46]. In fact, Mn^{2+} appears to be able to substitute for Zn^{2+} on the *S. pneumoniae* enzyme [34].

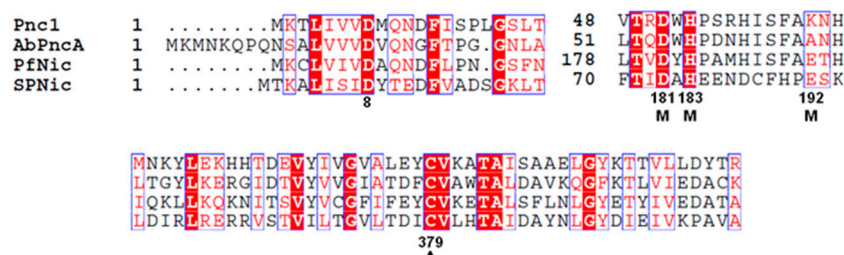


Figure 3. ClustalW alignment of the catalytic residues of nicotinamidases from *S. cerevisiae* (Pnc1), *A. baumannii* (AbPncA), *P. falciparum* (PfNic), and *S. pneumoniae* (SpNic). Identical residues are highlighted. The proposed metal binding residues are shown with an M underneath.

3.2. Expression and Characterization of PfNic

In PlasmDB, a gene producing a transcript called PFC0910w was cloned into a cloning vector. The transcript encodes a protein of predicted length of 429 amino acids (AAs) and molecular weight of 50.1 kDa. The typical nicotinamidase domain from most organisms is much shorter, comprising approximately 200 AAs, indicating that the *P. falciparum* enzyme might have an unusual structure. Subcloning into pet28a, which confers a histidine tag at the N-terminus, enabled protein expression in Rosetta (DE3) *E. coli* cells [34]. The isolated protein was purified to homogeneity by Ni-resin chromatography (Figure S1). Activity assay of this protein confirmed it to be a potent nicotinamidase, with steady state kinetic parameters of $K_m = 3.0 \pm 0.9 \mu M$ and $k_{cat} = 0.35 \pm 0.028 s^{-1}$ at pH 7, consistent with the previous report [34].

3.3. Identification of PfNic Inhibitors

In 1987, nicotinaldehyde was reported to be a weak inhibitor of the *S. cerevisiae* nicotinamidase, with a K_i value reported to be $68 \mu M$ [47]. This finding was later re-investigated to determine that nicotinaldehydes are general and very potent inhibitors of nicotinamidases [34]. These compounds form enzyme-stabilized hemithioacetals as proven on the *S. pneumoniae* nicotinamidase by X-ray crystallography [41]. The K_i values of nicotinaldehyde were found to be in the range 11–1400 nM for *S. pneumoniae*, *S. cerevisiae*, *P. falciparum*, *B. burgdorferi*, and two *C. elegans* enzymes [34]. The aldehyde

inhibitions were fully reversible and competitive with nicotinamide substrate [34]. A series of 3-pyridinecarboxaldehydes were synthesized and evaluated for their ability to inhibit nicotinamidases. These structure–activity relationship (SAR) studies have significantly improved our knowledge on the design and development of nicotinamidase inhibitors [34]. The small molecule nicotinamidase inhibitors provide new tools for the analysis of NAD⁺ biosynthetic pathways in *P. falciparum*. A potent lead compound, 5-methyl-nicotinaldehyde (5-Me-nicotinaldehyde), was chosen for further in vitro studies.

3.4. 5-Me-Nicotinaldehyde Inhibits PfNic Activity in *P. falciparum* Lysates

The function of PfNic is to proteolytically convert NAM to NA. By using carbonyl ¹⁴C-labeled NAM, this enzymatic hydrolysis can be monitored by HPLC and scintillation counting as described in Section 2. Using this assay, we found that *P. falciparum* lysates efficiently processed NAM (Figure 4). Furthermore, this activity can be blocked by pre-incubation of parasites with 50 μM 5-Me-nicotinaldehyde for 12 h (Figure 4). The mechanism of nicotinaldehyde inhibition is likely conserved for nicotinamidases and was established to occur via thiohemiacetal formation [34,41]. Inhibition by 5-Me-nicotinaldehyde suggests that NAM processing observed in parasite lysates is the result of active PfNic.

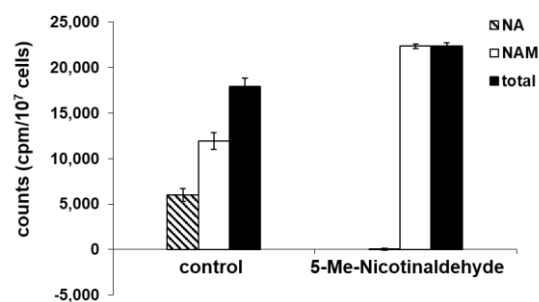


Figure 4. Inhibition of nicotinamidase in *P. falciparum* parasite lysate. Synchronized parasites were treated with or without 50 μM 5-Me-nicotinaldehyde for 12 h; harvested parasites were lysed and treated with 260,000 cpm of carbonyl ¹⁴C-nicotinamide for 30 min. NAM and NA were separated and collected by HPLC; radioactivity was determined by scintillation counting. For the drug treated parasites, there is no significant conversion of NAM to NA, indicating 5-Me-nicotinaldehyde was able to inhibit *P. falciparum* nicotinamidase in the lysate. Error bars represent S.D. of at least three biological replicates.

3.5. Nicotinamide Is the Preferred NAD⁺ Precursor in *P. falciparum*

The elucidation of NAD⁺ biosynthesis in cultured *P. falciparum* parasites is crucial to improve understanding of the feasibility of using inhibition of nicotinamidase as a strategy to prevent NAD⁺ biosynthesis and to control or prevent *P. falciparum* growth. Synchronized *P. falciparum* parasites growing in red blood cells (RBCs) in 20 mL culture volumes with 100 μM exogenously added NAM were incubated for 48 h (the blood stage *P. falciparum* typically demonstrates a 48 h life cycle) [48]. Percoll/sorbitol gradient separation allowed the recovery of 95% schizonts. NAD⁺ contents in these cells were measured by adding ¹⁸O-NAD⁺ and processed for MS analysis as reported previously [31,49,50]. The intensity of the peak for ¹⁸O-NAD⁺ (*m/z* = 666) was ratioed against peak of ¹⁶O-NAD⁺ (*m/z* = 664) in MALDI-MS to determine the NAD⁺ concentration in these cells to be 53 pmol/10⁶ cells. The NAD⁺ content was also determined in recovered uninfected RBCs to be 10.7 pmol/10⁶ cells. The 5 fold increase of NAD⁺ in the infected RBCs is in agreement with the report that *P. falciparum* causes an approximately 10 fold increase in NAD⁺ synthesis in infected RBCs [33].

To determine the percentage of NAD⁺ that is synthesized from NAM versus any other precursor, we used ¹⁵N labeled NAM as the source of isotopically labeled precursor. 1-¹⁵N-NAM (99%) and 1-¹⁵N-NA (99%) were synthesized as described before [51,52]. *P. falciparum* culture already contains 8.2 μM unlabeled NAM (in RPMI 1640) [53] and 10 μM unlabeled NA (an ingredient in Albumax II as determined by us, Figure S2). We supplemented the media with either 100 μM unlabeled NAM or 100 μM ¹⁵N-NAM (Figure 5A). The

highest intensity peak in each case was normalized to be 100; the ratio of 664 peak to 665 peak reflects the relative amount of NAD^+ vs. $^{15}\text{N-NAD}^+$. When treated with regular NAM, the intensity of 665 peak is minimal which represents the natural abundance of this isotopomer. After 48 h, the $^{15}\text{N-NAM}$ treated cells have nearly 80% ^{15}N incorporation in NAD^+ , indicating $^{15}\text{N-NAM}$ is the dominant precursor for NAD^+ biosynthesis under these conditions. When parasites were treated with $20\ \mu\text{M}$ $^{15}\text{N-NA}$ and $20\ \mu\text{M}$ unlabeled NAM, NAD^+ levels remained at $50\ \text{pmol}/10^6$ cells without significant incorporation of ^{15}N was observed (Figure S3). These data support the hypothesis that NAM is the dominant source of *P. falciparum* NAD^+ in culture.

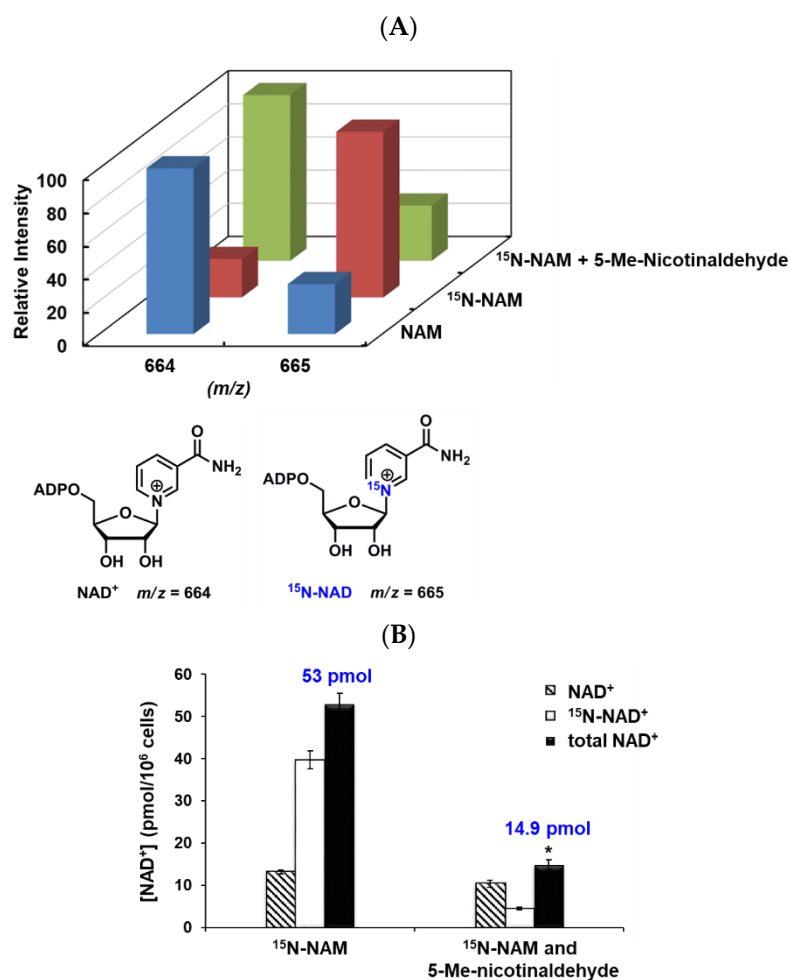


Figure 5. NAM is the preferred precursor for *P. falciparum* NAD^+ biosynthesis. (A) Relative intensity of NAD^+ isotopomers from parasite culture treated with $100\ \mu\text{M}$ NAM, $100\ \mu\text{M}$ $^{15}\text{N-NAM}$, or $100\ \mu\text{M}$ $^{15}\text{N-NAM}$ and $50\ \mu\text{M}$ 5-Me-nicotinaldehyde for 48 h. NAD^+ levels were determined by MALDI-MS. The chemical structures of NAD^+ and $^{15}\text{N-NAD}^+$ are shown below. (B) The addition of 5-Me-nicotinaldehyde, a nanomolar inhibitor of *P. falciparum* nicotinamidase, decreased the conversion of $^{15}\text{N-NAM}$ to $^{15}\text{N-NAD}^+$ to only 10% of inhibitor free sample. Addition of the inhibitor also caused total NAD^+ level to decrease from $53\ \text{pmol}/10^6$ cells to $14.9\ \text{pmol}/10^6$ cells (* $p = 0.003$). Error bars represent S.D. of at least three biological replicates.

3.6. Inhibition of NAD^+ Biosynthesis by Nicotinamidase Inhibitors Can Be Reversed by Nicotinic Acid

To test if an inhibitor of *P. falciparum* nicotinamidase could decrease the conversion of NAM to NAD^+ , we incubated the parasites with $100\ \mu\text{M}$ $^{15}\text{N-NAM}$ with or without $50\ \mu\text{M}$ 5-Me-nicotinaldehyde. As shown in Figure 5B, the presence of PfNic inhibitor caused 90% loss of ^{15}N incorporation in NAD^+ . Although recovered cell counts after 48 h were similar for both groups, the inhibitor treated parasites experienced a statistically significant

loss of NAD⁺ down to only 28% of controls ($p = 0.003$, Figure 5B). These suggested that *P. falciparum* is highly dependent upon nicotinamide for NAD⁺ homeostasis and that interference with this enzyme can cause acute depletion of NAD⁺ level.

Furthermore, in order to rule out the possibility of off-target effect and to determine if a defect in NAD⁺ biosynthesis can be rescued by a downstream metabolite, parasites were treated with either vehicle (DMSO), or 50 μM 5-Me-nicotinaldehyde, or a combination of 50 μM 5-Me-nicotinaldehyde and 100 μM ¹⁵N-NA. Indeed, the significant decrease of NAD⁺ concentration upon inhibitor administration was rescued by the addition of a high dose of NA with 81% ¹⁵N incorporation in NAD⁺ (Figure 6). These experiments allowed us to assess the specific repressive effect of PfNic inhibitor on NAD⁺ level. The disrupted NAD⁺ homeostasis can be corrected with another NAD⁺ precursor, namely, NA.

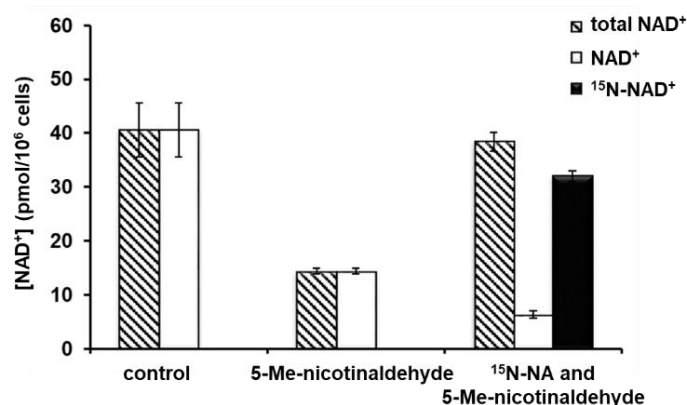


Figure 6. The disrupted NAD⁺ homeostasis through inhibition of nicotinamide can be corrected with nicotinic acid. NAD⁺, ¹⁵N-NAD⁺, and total NAD⁺ levels in parasites treated with vehicle (DMSO), 50 μM 5-Me-nicotinaldehyde, or a combination of 50 μM 5-Me-nicotinaldehyde and 100 μM ¹⁵N-NA. The significant decrease of NAD⁺ concentration upon inhibitor administration was rescued by the addition of ¹⁵N-NA with 81% ¹⁵N incorporation in NAD⁺. Error bars represent S.D. of at least three biological replicates.

3.7. Nicotinaldehydes Inhibits *P. falciparum* Replication

5-Br-nicotinaldehyde was tested for its ability to inhibit chloroquine-sensitive *P. falciparum* strain 3D7 growth using both the *Renilla*-luciferase assay [54] to measure parasites viability, and microscopic examination of morphological changes. Although the compound did not significantly affect parasite's growth at moderate concentrations ($\text{IC}_{50} = 643.7 \mu\text{M}$) (Figure 7A), it did exert inhibitory effect on NAD⁺ level (Figure S4). We reasoned that the presence of 10 μM NA in regular culture medium (0.5% Albumax II) could rescue the metabolic block induced by PfNic inhibitors. Reducing NA level down to 2 μM in culture media (0.1% Albumax II) did not affect normal growth in the 48 h time frame (Figure S5). With reduced Albumax II content, the incubation with 200 μM 5-Br-nicotinaldehyde completely blocked host cell escape and reinvasion by arresting parasites in the ring growth stage (Figure S6). The more potent compound, 5-Me-nicotinaldehyde with an IC_{50} value of 9.09 μM (Figure 7B), demonstrated a similar effect at 10 μM (Figure 8), and more importantly, this growth arrest can be reversed with the addition of 100 μM NA. These data confirm that depletion of NAD⁺ is detrimental to *P. falciparum*, and inhibition of PfNic is indeed effective to block parasite replication. It is important to note that the IC_{50} values of the inhibitors may be altered in response to different Albumax II contents (different NA concentrations).

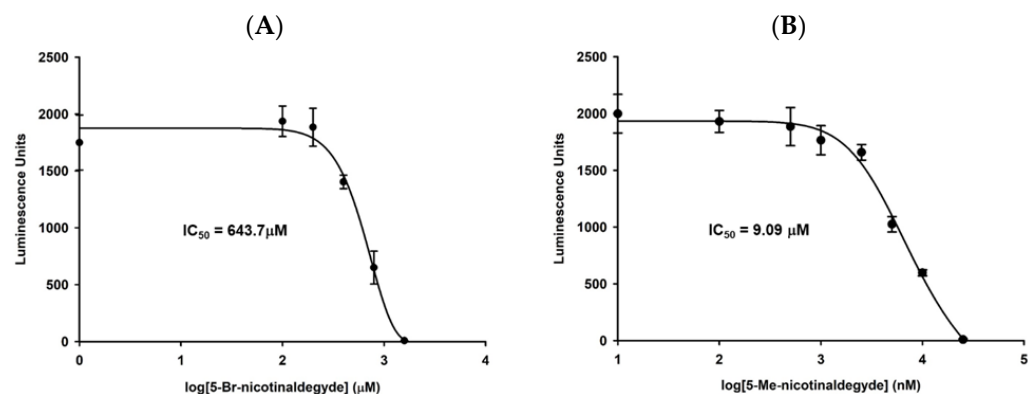


Figure 7. Viability assay for parasites treated with nicotinaldehyde derivatives. 3D7 Parasites (chloroquine-sensitive) were plated at 1–10% parasitemia in 96-well plates in standard media in the presence of the indicated concentrations of inhibitor. The total volume of culture was 200 μL , and DMSO did not exceed 1% of the total culture volume. Media plus compounds were replenished every 12 h. After 48 h incubation, media were withdrawn and RBCs were lysed with 100 μL of Bright-Glo Lysis Buffer (Promega, Madison, WI, USA). Lysates were then transferred to 96-well luminometer plates. To the lysates were added 100 μL of Bright-Glo *Renilla* Luciferase Reagent (Promega, Madison, WI, USA), luminescence was measured immediately in a plate luminometer (Molecular Devices). Each individual data point is represented in triplicate allowing determination of standard deviations. A broad range of compound concentrations are used to allow the determination of IC₅₀ value to be 643.7 μM for 5-Br-nicotinaldehyde (A), and 9.09 μM for 5-Me-nicotinaldehyde (B), respectively. Error bars represent S.D. of two independent experiments in triplicates.

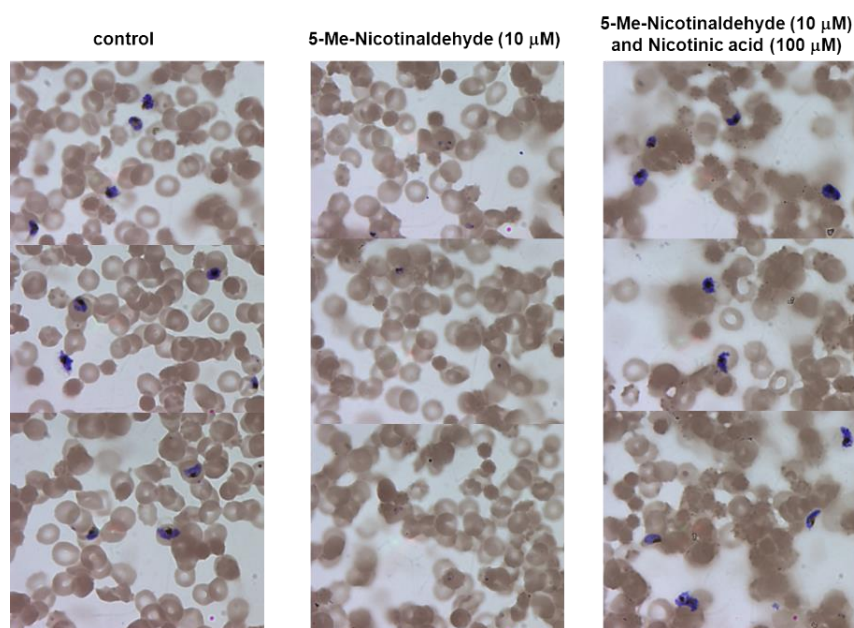


Figure 8. Inhibitory effect of 5-Me-nicotinaldehyde *in vitro*. Images of Giemsa-stained blood smears from synchronously grown parasites cultures treated with DMSO (control), 10 μM 5-Me-nicotinaldehyde or 10 μM 5-Me-nicotinaldehyde plus 100 μM NA. Smears were taken 48 h after the addition of the compound. Culture media contained only 0.1% Albumax II, this would reduce the nicotinic acid level in the media down to 2 μM . *PfNic* inhibitor caused growth arrest of parasites in the ring stage, this arrest can be reversed with the addition of NA. The treatments were repeated in three biological replicates.

4. Discussion and Conclusions

The idea that nicotinamidase could represent an attractive antimicrobial target in pathogens that infect humans is supported by genetic studies [55–57]. In organisms with NAD⁺ metabolism similar to *P. falciparum*, the loss of nicotinamidase achieved by genetic deletion caused loss of virulence, infectivity and proliferative capability. For example, *Brucella abortus* infects phagocytes and lives within them [56,58]. These are gram negative bacteria and cause chronic infections, in part because of their intracellular lifecycle, which enables them to evade host immunity. *B. abortus* lacks a de novo NAD⁺ biosynthetic pathway. It has nicotinamidase, nicotinate mononucleotide adenylyltransferase (NMNAT), nicotinamide phosphoribosyltransferase (NAMPT), and NAD⁺ synthetase genes, similar to what has been found for *P. falciparum*. Removal of the nicotinamidase gene (*PNCA*) from *B. abortus*, one of four *Brucella* species known to infect humans, causes a nearly complete failure in intracellular replication in culture unless media are supplemented with NA. [59]. Similarly, growth in macrophages is strongly attenuated in *PNCA*[−] bacteria [59]. *PNCA*[−] bacteria cause an appropriate immune response suggesting *PNCA* deletion may represent a means for an attenuated live vaccine for *Brucella* [59]. These examples emphasize the likelihood that nicotinamidase inhibitors could represent viable compounds to limit pathogen growth and virulence in humans, providing data in support of the idea that targeted inhibition of nicotinamidase in organisms such as *P. falciparum*, which have similarly configured NAD⁺ biosynthetic pathways, could represent an effective yet unexplored therapeutic approach.

Up until recently, both the catalytic mechanism and the structural organization of the active sites of nicotinamidases were essentially unknown, and there were no known general inhibitors of these enzymes. This situation has changed with the development of a continuous assay for nicotinamidase activity, the identification of nicotinaldehydes as potent and general mechanism-based inhibitors of nicotinamidases, and the X-ray crystal structural studies of liganded nicotinamidases [34,41]. These recent findings have clarified important features of the active site design and crucial aspects of the catalytic mechanism.

The *P. falciparum* nicotinamidase was cloned and functionally expressed. Kinetic properties of this enzyme along with inhibitions by nicotinaldehydes have been reported [34]. In this study, we demonstrated that 5-Me-nicotinaldehyde inhibits *PfNic* activity in parasite lysates. To monitor the metabolites utilization by the parasites, we employed isotopically labeled NAD⁺ precursors and used NAD⁺ levels and isotope abundance as readouts. 5-Me-nicotinaldehyde causes dramatic reduction of the incorporation of NAM into NAD⁺ and significant depletion of NAD⁺ level in parasite cultured in human RBCs. This reduction can be restored by a high concentration of NA. These studies not only elucidate the NAM salvage pathway in *P. falciparum* but also support the hypothesis that NAM is the preferred precursor for NAD⁺ along this pathway.

An important assumption about the effectiveness of nicotinamidase inhibition as a potential antimalarial approach is the limited availability and bioactivity of NA in the body. Indeed, although nicotinaldehydes showed an inhibitory effect on NAD⁺ concentrations and dose-dependent inhibition of parasites growth, these effects were not sufficient to fully block parasite replication in our initial tests. Only when nicotinic acid level was reduced by 80% in the culture medium, in other words, the availability of alternative NAD⁺ precursor was minimized, growth arrests were observed upon inhibitor treatment. In human serum, the NA level is around 0.1~1 μM [60,61]. Dietary NA derives mostly from plant foods, is converted to NAD⁺ predominantly in the intestine and liver, and is released to the rest of the body from the liver in the form of NAM [62,63]. For erythrocytes that harbor *P. falciparum* parasites, measurements suggest such low concentrations of NA in these cells that they are virtually undetectable. The cumulative amount of NaMN and NaAD is only 6 μM, whereas NMN and NAD⁺ levels cumulatively represent 400 μM [64], suggesting that NAM is likely the most available source for the pyridine-3-carboxy moiety for *P. falciparum* in the host.

The nicotinamidases from the species *P. berghei* and *P. yoelii* exhibit 53% identity to PfNic (Figure S7). Thus, it could be possible to have new antimalarial drugs that are effective against major species of *Plasmodium* by targeting nicotinamidases.

Cells under stress due to treatment with antibiotics or chemotherapeutic drugs often require increased NAD⁺ levels for recovery. Thus, compounds that reduce NAD⁺ production often act synergistically with drugs that target other, unrelated metabolic pathways. This is particularly true for drugs that are known to release reactive radicals or cause oxidative damage inside the cell. Several antimalarial drugs, including chloroquine, mefloquine, and quinine, are thought to cause extensive oxidative damage by disrupting heme polymerization [65]. There is a high probability that reducing NAD⁺ levels in the cells will make the parasites hypersensitive to these compounds. Therefore, nicotinamidase inhibitors might act synergistically with these drugs in treating malaria.

The action of nicotinamidases on NAD⁺ levels inside parasites can have profound effects on gene expression. The *P. falciparum* genome contains two *sir2* genes that encode partially redundant versions of the protein SIR2 [66]. Knockouts of either of these genes result in down-regulation of the overall level of SIR2 activity in the cell and lead to significant de-silencing of large portions of the *var* gene family [67,68]. Each *var* gene encodes a different variant of the surface protein erythrocyte membrane protein 1 (PfEMP1), the primary virulence determinant of *P. falciparum*. The parasite genome contains 60 *var* gene copies, with all but a single gene maintained in a silent state, at least in part through the action of SIR2. It is important for each parasite to only express one *var* gene at a time, and to switch expression over the length of an infection to enable it to avoid the host's antibody response against previously expressed *var* gene products [69]. The parasite's ability to maintain a chronic infection is dependent on this coordinated gene expression pattern, and disruption of *var* gene silencing would expose the entire antigen repertoire to the host prematurely, thus effectively "vaccinating" the infected individual against all variants of the parasite. Disruption of silencing of an analogous gene family in the intestinal parasite *Giardia lamblia* did indeed result in the effective vaccination of infected mice [70], lending support for the potential efficacy of this strategy. Since treatment with nicotinamidase inhibitors results in drastic reduction in NAD⁺ levels, it is likely that SIR2 activity will be reduced correspondingly and that *var* gene silencing might be disrupted. All of these await further investigation.

Supplementary Materials: The following supporting information can be downloaded at: <https://www.mdpi.com/article/10.3390/biom12081109/s1>, Figure S1: SDS-PAGE of purified PfNic; Figure S2: *P. falciparum* culture medium contains NA; Figure S3: NA is not the preferred NAD biosynthetic precursor for *P. falciparum*; Figure S4: 5-Br-nicotinaldehyde reduces *P. falciparum* NAD⁺ levels; Figure S5: Reduced Albumax II concentration does not affect parasite growth; Figure S6: Inhibitory effect of 5-Br-nicotinaldehyde *in vitro*; Figure S7: Sequence alignment of nicotinamidases from *P. Berghei*, *P. Yoelii*, and *P. falciparum*.

Author Contributions: Conceptualization, Y.C.; methodology, D.D., C.S. and Y.C.; formal analysis, D.D., C.S. and Y.C.; investigation, D.D., C.S. and Y.C.; writing—original draft preparation, D.D., C.S. and Y.C.; writing—review and editing, D.D., C.S. and Y.C.; funding acquisition, Y.C. All authors have read and agreed to the published version of the manuscript.

Funding: This work was supported in part by Jeffress Trust Award in Interdisciplinary Research from Thomas F. and Kate Miller Jeffress Memorial Trust and Bank of America (to Y.C.), Presidential Research Quest Fund from VCU (to Y.C.), and 1R01GM143176-01A1 from NIH/NIGMS (to Y.C.).

Institutional Review Board Statement: Not applicable.

Informed Consent Statement: Not applicable.

Data Availability Statement: Not applicable.

Conflicts of Interest: The authors declare no conflict of interest.

References

1. Magni, G.; Amici, A.; Emanuelli, M.; Raffaelli, N.; Ruggieri, S. Enzymology of NAD⁺ synthesis. *Adv. Enzymol. Relat. Areas Mol. Biol.* **1999**, *73*, 135–182.
2. Shats, I.; Williams, J.G.; Liu, J.; Makarov, M.V.; Wu, X.; Lih, F.B.; Deterding, L.J.; Lim, C.; Xu, X.; Randall, T.A.; et al. Bacteria Boost Mammalian Host NAD Metabolism by Engaging the Deamidated Biosynthesis Pathway. *Cell Metab.* **2020**, *31*, 564–579.e7. [[CrossRef](#)] [[PubMed](#)]
3. Sauve, A.A. NAD⁺ and vitamin B3: From metabolism to therapies. *J. Pharmacol. Exp. Ther.* **2008**, *324*, 883–893. [[CrossRef](#)]
4. Begley, T.P.; Kinsland, C.; Mehl, R.A.; Osterman, A.; Dorrestein, P. The biosynthesis of nicotinamide adenine dinucleotides in bacteria. *Vitam. Horm.* **2001**, *61*, 103–119.
5. Kurnasov, O.; Goral, V.; Colabroy, K.; Gerdes, S.; Anantha, S.; Osterman, A.; Begley, T.P. NAD biosynthesis: Identification of the tryptophan to quinolinate pathway in bacteria. *Chem. Biol.* **2003**, *10*, 1195–1204. [[CrossRef](#)] [[PubMed](#)]
6. Gazzaniga, F.; Stebbins, R.; Chang, S.Z.; McPeck, M.A.; Brenner, C. Microbial NAD metabolism: Lessons from comparative genomics. *Microbiol. Mol. Biol. Rev.* **2009**, *73*, 529–541. [[CrossRef](#)]
7. Belenky, P.; Bogan, K.L.; Brenner, C. NAD⁺ metabolism in health and disease. *Trends Biochem. Sci.* **2007**, *32*, 12–19. [[CrossRef](#)]
8. Bogan, K.L.; Brenner, C. Nicotinic acid, nicotinamide, and nicotinamide riboside: A molecular evaluation of NAD⁺ precursor vitamins in human nutrition. *Annu. Rev. Nutr.* **2008**, *28*, 115–130. [[CrossRef](#)]
9. Chauhan, N.; Poddar, R. In silico pharmacophore modeling and simulation studies for searching potent antileishmanials targeted against *Leishmania donovani* nicotinamidase. *Comput. Biol. Chem.* **2019**, *83*, 107150. [[CrossRef](#)] [[PubMed](#)]
10. Shang, F.; Chen, J.; Wang, L.; Jin, L.; Zou, L.; Bu, T.; Dong, Y.; Ha, N.C.; Nam, K.H.; Quan, C.; et al. Crystal structure of the nicotinamidase/pyrazinamidase PncA from *Bacillus subtilis*. *Biochem. Biophys. Res. Commun.* **2018**, *503*, 2906–2911. [[CrossRef](#)] [[PubMed](#)]
11. Curry, A.; White, D.; Cen, Y. Small Molecule Regulators Targeting NAD(+) Biosynthetic Enzymes. *Curr. Med. Chem.* **2022**, *29*, 1718–1738. [[CrossRef](#)] [[PubMed](#)]
12. Osterman, A.L.; Rodionova, I.; Li, X.; Sergienko, E.; Ma, C.T.; Catanzaro, A.; Pettigrove, M.E.; Reed, R.W.; Gupta, R.; Rohde, K.H.; et al. Novel Antimycobacterial Compounds Suppress NAD Biogenesis by Targeting a Unique Pocket of NaMN Adenylyltransferase. *ACS Chem. Biol.* **2019**, *14*, 949–958. [[CrossRef](#)] [[PubMed](#)]
13. Rodionova, I.A.; Zuccola, H.J.; Sorci, L.; Aleshin, A.E.; Kazanov, M.D.; Ma, C.T.; Sergienko, E.; Rubin, E.J.; Locher, C.P.; Osterman, A.L. Mycobacterial nicotinate mononucleotide adenylyltransferase: Structure, mechanism, and implications for drug discovery. *J. Biol. Chem.* **2015**, *290*, 7693–7706. [[CrossRef](#)] [[PubMed](#)]
14. Wang, X.; Ahn, Y.M.; Lentscher, A.G.; Lister, J.S.; Brothers, R.C.; Kneen, M.M.; Gerratana, B.; Boshoff, H.I.; Dowd, C.S. Design, synthesis, and evaluation of substituted nicotinamide adenine dinucleotide (NAD⁺) synthetase inhibitors as potential antitubercular agents. *Bioorg. Med. Chem. Lett.* **2017**, *27*, 4426–4430. [[CrossRef](#)]
15. Teixeira, C.S.S.; Cerqueira, N.; Sousa, S.F. Multifunctional Enzymes as Targets for the Treatment of Tuberculosis: Paving the Way for New Anti-TB Drugs. *Curr. Med. Chem.* **2021**, *28*, 5847–5882. [[CrossRef](#)]
16. Wang, T.; Zhang, X.; Bheda, P.; Revollo, J.R.; Imai, S.; Wolberger, C. Structure of Nampt/PBEF/visfatin, a mammalian NAD⁺ biosynthetic enzyme. *Nat. Struct. Mol. Biol.* **2006**, *13*, 661–662. [[CrossRef](#)] [[PubMed](#)]
17. Dietrich, L.S.; Fuller, L.; Yero, I.L.; Martinez, L. Nicotinamide mononucleotide pyrophosphorylase activity in animal tissues. *J. Biol. Chem.* **1966**, *241*, 188–191. [[CrossRef](#)]
18. Preiss, J.; Handler, P. Biosynthesis of diphosphopyridine nucleotide. I. Identification of intermediates. *J. Biol. Chem.* **1958**, *233*, 488–492. [[CrossRef](#)]
19. Xu, P.; Sauve, A.A. Vitamin B3, the nicotinamide adenine dinucleotides and aging. *Mech. Ageing Dev.* **2010**, *131*, 287–298. [[CrossRef](#)]
20. Geleta, G.; Ketema, T.; Severe, M. Associated with *Plasmodium falciparum* and *P. vivax* among Children in Pawe Hospital, Northwest Ethiopia. *Malar. Res. Treat.* **2016**, *2016*, 1240962. [[CrossRef](#)]
21. Florini, F.; Visone, J.E.; Deitsch, K.W. Shared Mechanisms for Mutually Exclusive Expression and Antigenic Variation by Protozoan Parasites. *Front. Cell Dev. Biol.* **2022**, *10*, 852239. [[CrossRef](#)]
22. Sakoguchi, A.; Arase, H. Mechanisms for Host Immune Evasion Mediated by *Plasmodium falciparum*-Infected Erythrocyte Surface Antigens. *Front. Immunol.* **2022**, *13*, 901864. [[CrossRef](#)]
23. Tchekounou, C.; Zida, A.; Zongo, C.; Soulama, I.; Sawadogo, P.M.; Guiguemde, K.T.; Sangare, I.; Guiguemde, R.T.; Traore, Y. Antimalarial drugs resistance genes of *Plasmodium falciparum*: A review. *Ann. Parasitol.* **2022**, *68*, 215–225.
24. Gil, J.P.; Fancony, C. *Plasmodium falciparum* Multidrug Resistance Proteins (pfMRPs). *Front. Pharmacol.* **2021**, *12*, 759422. [[CrossRef](#)]
25. Rasmussen, C.; Alonso, P.; Ringwald, P. Current and emerging strategies to combat antimalarial resistance. *Expert Rev. Anti. Infect. Ther.* **2022**, *20*, 353–372. [[CrossRef](#)]
26. *Guidelines for the Treatment of Malaria*, 3rd ed.; World Health Organization: Geneva, Switzerland, 2015.
27. Tisnerat, C.; Dassonville-Klimpt, A.; Gosselet, F.; Sonnet, P. Antimalarial Drug Discovery: From Quinine to the Most Recent Promising Clinical Drug Candidates. *Curr. Med. Chem.* **2022**, *29*, 3326–3365. [[CrossRef](#)]
28. Miller, L.H.; Baruch, D.I.; Marsh, K.; Doumbo, O.K. The pathogenic basis of malaria. *Nature* **2002**, *415*, 673–679. [[CrossRef](#)]

29. Buffet, P.A.; Safeukui, I.; Deplaine, G.; Brousse, V.; Prendki, V.; Thellier, M.; Turner, G.D.; Mercereau-Puijalon, O. The pathogenesis of *Plasmodium falciparum* malaria in humans: Insights from splenic physiology. *Blood* **2011**, *117*, 381–392. [[CrossRef](#)]
30. Plata, G.; Hsiao, T.L.; Olszewski, K.L.; Llinas, M.; Vitkup, D. Reconstruction and flux-balance analysis of the *Plasmodium falciparum* metabolic network. *Mol. Syst. Biol.* **2010**, *6*, 408. [[CrossRef](#)]
31. Fulco, M.; Cen, Y.; Zhao, P.; Hoffman, E.P.; McBurney, M.W.; Sauve, A.A.; Sartorelli, V. Glucose restriction inhibits skeletal myoblast differentiation by activating SIRT1 through AMPK-mediated regulation of Nampt. *Dev. Cell* **2008**, *14*, 661–673. [[CrossRef](#)]
32. Trammell, S.A.; Schmidt, M.S.; Weidemann, B.J.; Redpath, P.; Jaksch, F.; Dellinger, R.W.; Li, Z.; Abel, E.D.; Migaud, M.E.; Brenner, C. Nicotinamide riboside is uniquely and orally bioavailable in mice and humans. *Nat. Commun.* **2016**, *7*, 12948. [[CrossRef](#)] [[PubMed](#)]
33. Zerez, C.R.; Roth, E.F., Jr.; Schulman, S.; Tanaka, K.R. Increased nicotinamide adenine dinucleotide content and synthesis in *Plasmodium falciparum*-infected human erythrocytes. *Blood* **1990**, *75*, 1705–1710. [[CrossRef](#)] [[PubMed](#)]
34. French, J.B.; Cen, Y.; Vrablik, T.L.; Xu, P.; Allen, E.; Hanna-Rose, W.; Sauve, A.A. Characterization of nicotinamidases: Steady state kinetic parameters, classwide inhibition by nicotinaldehydes, and catalytic mechanism. *Biochemistry* **2010**, *49*, 10421–10439. [[CrossRef](#)] [[PubMed](#)]
35. Swamy, L.; Amulic, B.; Deitsch, K.W. *Plasmodium falciparum* var gene silencing is determined by cis DNA elements that form stable and heritable interactions. *Eukaryot. Cell* **2011**, *10*, 530–539. [[CrossRef](#)] [[PubMed](#)]
36. Radfar, A.; Mendez, D.; Moneriz, C.; Linares, M.; Marin-Garcia, P.; Puyet, A.; Diez, A.; Bautista, J.M. Synchronous culture of *Plasmodium falciparum* at high parasitemia levels. *Nat. Protoc.* **2009**, *4*, 1899–1915. [[CrossRef](#)]
37. Bai, P.; Canto, C.; Brunyanszki, A.; Huber, A.; Szanto, M.; Cen, Y.; Yamamoto, H.; Houten, S.M.; Kiss, B.; Oudart, H.; et al. PARP-2 regulates SIRT1 expression and whole-body energy expenditure. *Cell Metab.* **2011**, *13*, 450–460. [[CrossRef](#)]
38. North, B.J.; Rosenberg, M.A.; Jeganathan, K.B.; Hafner, A.V.; Michan, S.; Dai, J.; Baker, D.J.; Cen, Y.; Wu, L.E.; Sauve, A.A.; et al. SIRT2 induces the checkpoint kinase BubR1 to increase lifespan. *EMBO J.* **2014**, *33*, 1438–1453. [[CrossRef](#)]
39. Yang, Y.; Sauve, A.A. Assays for Determination of Cellular and Mitochondrial NAD(+) and NADH Content. *Methods Mol. Biol.* **2021**, *2310*, 271–285.
40. Epp, C.; Raskolnikov, D.; Deitsch, K.W. A regulatable transgene expression system for cultured *Plasmodium falciparum* parasites. *Malar. J.* **2008**, *7*, 86. [[CrossRef](#)]
41. French, J.B.; Cen, Y.; Sauve, A.A.; Ealick, S.E. High-resolution crystal structures of *Streptococcus pneumoniae* nicotinamidase with trapped intermediates provide insights into the catalytic mechanism and inhibition by aldehydes. *Biochemistry* **2010**, *49*, 8803–8812. [[CrossRef](#)]
42. Fyfe, P.K.; Rao, V.A.; Zemla, A.; Cameron, S.; Hunter, W.N. Specificity and mechanism of *Acinetobacter baumannii* nicotinamidase: Implications for activation of the front-line tuberculosis drug pyrazinamide. *Angew. Chem. Int. Ed. Engl.* **2009**, *48*, 9176–9179. [[CrossRef](#)] [[PubMed](#)]
43. Zhang, H.; Deng, J.Y.; Bi, L.J.; Zhou, Y.F.; Zhang, Z.P.; Zhang, C.G.; Zhang, Y.; Zhang, X.E. Characterization of *Mycobacterium tuberculosis* nicotinamidase/pyrazinamidase. *FEBS J.* **2008**, *275*, 753–762. [[CrossRef](#)] [[PubMed](#)]
44. Hu, G.; Taylor, A.B.; McAlister-Henn, L.; Hart, P.J. Crystal structure of the yeast nicotinamidase Pnc1p. *Arch. Biochem. Biophys.* **2007**, *461*, 66–75. [[CrossRef](#)] [[PubMed](#)]
45. Du, X.; Wang, W.; Kim, R.; Yakota, H.; Nguyen, H.; Kim, S.H. Crystal structure and mechanism of catalysis of a pyrazinamidase from *Pyrococcus horikoshii*. *Biochemistry* **2001**, *40*, 14166–14172. [[CrossRef](#)]
46. Seiner, D.R.; Hegde, S.S.; Blanchard, J.S. Kinetics and inhibition of nicotinamidase from *Mycobacterium tuberculosis*. *Biochemistry* **2010**, *49*, 9613–9619. [[CrossRef](#)]
47. Yan, C.; Sloan, D.L. Purification and characterization of nicotinamide deamidase from yeast. *J. Biol. Chem.* **1987**, *262*, 9082–9087. [[CrossRef](#)]
48. Sato, S. *Plasmodium*-a brief introduction to the parasites causing human malaria and their basic biology. *J. Physiol. Anthropol.* **2021**, *40*, 1. [[CrossRef](#)]
49. Tran, A.; Yokose, R.; Cen, Y. Chemo-enzymatic synthesis of isotopically labeled nicotinamide riboside. *Org. Biomol. Chem.* **2018**, *16*, 3662–3671. [[CrossRef](#)]
50. Curry, A.M.; Barton, E.; Kang, W.; Mongeluzi, D.V.; Cen, Y. Development of Second Generation Activity-Based Chemical Probes for Sirtuins. *Molecules* **2020**, *26*, 11. [[CrossRef](#)]
51. Rising, K.A.; Schramm, V.L. Enzymatic-Synthesis of Nad(+) with the Specific Incorporation of Atomic Labels. *J. Am. Chem. Soc.* **1994**, *116*, 6531–6536. [[CrossRef](#)]
52. Cen, Y.; Sauve, A.A. Transition state of ADP-ribosylation of acetyllysine catalyzed by *Archaeoglobus fulgidus* Sir2 determined by kinetic isotope effects and computational approaches. *J. Am. Chem. Soc.* **2010**, *132*, 12286–12298. [[CrossRef](#)]
53. Moore, G.E.; Gerner, R.E.; Franklin, H.A. Culture of normal human leukocytes. *JAMA* **1967**, *199*, 519–524. [[CrossRef](#)] [[PubMed](#)]
54. Merckx, A.; Nivez, M.P.; Bouyer, G.; Alano, P.; Langsley, G.; Deitsch, K.; Thomas, S.; Doerig, C.; Egee, S. *Plasmodium falciparum* regulatory subunit of cAMP-dependent PKA and anion channel conductance. *PLoS Pathog.* **2008**, *4*, e19. [[CrossRef](#)] [[PubMed](#)]
55. Gygli, S.M.; Borrell, S.; Trauner, A.; Gagneux, S. Antimicrobial resistance in *Mycobacterium tuberculosis*: Mechanistic and evolutionary perspectives. *FEMS Microbiol. Rev.* **2017**, *41*, 354–373. [[CrossRef](#)] [[PubMed](#)]
56. Gorvel, J.P. *Brucella*: A Mr “Hide” converted into Dr Jekyll. *Microbes Infect.* **2008**, *10*, 1010–1013. [[CrossRef](#)]

57. Zapata-Perez, R.; Garcia-Saura, A.G.; Jebbar, M.; Golyshin, P.N.; Sanchez-Ferrer, A. Combined Whole-Cell High-Throughput Functional Screening for Identification of New Nicotinamidases/Pyrazinamidases in Metagenomic/Polygenomic Libraries. *Front. Microbiol.* **2016**, *7*, 1915. [[CrossRef](#)]
58. Pizarro-Cerda, J.; Meresse, S.; Parton, R.G.; van der Goot, G.; Sola-Landa, A.; Lopez-Goni, I.; Moreno, E.; Gorvel, J.P. Brucella abortus transits through the autophagic pathway and replicates in the endoplasmic reticulum of nonprofessional phagocytes. *Infect. Immun.* **1998**, *66*, 5711–5724. [[CrossRef](#)]
59. Kim, S.; Kurokawa, D.; Watanabe, K.; Makino, S.; Shirahata, T.; Watarai, M. Brucella abortus nicotinamidase (PncA) contributes to its intracellular replication and infectivity in mice. *FEMS Microbiol. Lett.* **2004**, *234*, 289–295. [[CrossRef](#)]
60. Garcia, C.K.; Brown, M.S.; Pathak, R.K.; Goldstein, J.L. cDNA cloning of MCT2, a second monocarboxylate transporter expressed in different cells than MCT1. *J. Biol. Chem.* **1995**, *270*, 1843–1849. [[CrossRef](#)]
61. Spector, R. Niacin and niacinamide transport in the central nervous system. In vivo studies. *J. Neurochem.* **1979**, *33*, 895–904. [[CrossRef](#)] [[PubMed](#)]
62. Kirkland, J.B. Niacin status impacts chromatin structure. *J. Nutr.* **2009**, *139*, 2397–2401. [[CrossRef](#)] [[PubMed](#)]
63. Kirkland, J.B. Niacin status, NAD distribution and ADP-ribose metabolism. *Curr. Pharm. Des.* **2009**, *15*, 3–11. [[CrossRef](#)]
64. Yamada, K.; Hara, N.; Shibata, T.; Osago, H.; Tsuchiya, M. The simultaneous measurement of nicotinamide adenine dinucleotide and related compounds by liquid chromatography/electrospray ionization tandem mass spectrometry. *Anal. Biochem.* **2006**, *352*, 282–285. [[CrossRef](#)]
65. Sullivan, D.J., Jr.; Gluzman, I.Y.; Russell, D.G.; Goldberg, D.E. On the molecular mechanism of chloroquine's antimalarial action. *Proc. Natl. Acad. Sci. USA* **1996**, *93*, 11865–11870. [[CrossRef](#)]
66. Gardner, M.J.; Hall, N.; Fung, E.; White, O.; Berriman, M.; Hyman, R.W.; Carlton, J.M.; Pain, A.; Nelson, K.E.; Bowman, S.; et al. Genome sequence of the human malaria parasite Plasmodium falciparum. *Nature* **2002**, *419*, 498–511. [[CrossRef](#)]
67. Duraisingh, M.T.; Voss, T.S.; Marty, A.J.; Duffy, M.F.; Good, R.T.; Thompson, J.K.; Freitas-Junior, L.H.; Scherf, A.; Crabb, B.S.; Cowman, A.F. Heterochromatin silencing and locus repositioning linked to regulation of virulence genes in Plasmodium falciparum. *Cell* **2005**, *121*, 13–24. [[CrossRef](#)] [[PubMed](#)]
68. Tonkin, C.J.; Carret, C.K.; Duraisingh, M.T.; Voss, T.S.; Ralph, S.A.; Hommel, M.; Duffy, M.F.; Silva, L.M.; Scherf, A.; Ivens, A.; et al. Sir2 paralogs cooperate to regulate virulence genes and antigenic variation in Plasmodium falciparum. *PLoS Biol.* **2009**, *7*, e84. [[CrossRef](#)] [[PubMed](#)]
69. Dzikowski, R.; Deitsch, K.W. Genetics of antigenic variation in Plasmodium falciparum. *Curr. Genet.* **2009**, *55*, 103–110. [[CrossRef](#)] [[PubMed](#)]
70. Rivero, F.D.; Saura, A.; Prucca, C.G.; Carranza, P.G.; Torri, A.; Lujan, H.D. Disruption of antigenic variation is crucial for effective parasite vaccine. *Nat. Med.* **2010**, *16*, 551–557. [[CrossRef](#)]